

Optical and structural characterization of r.f. sputtered CeO₂ thin films

R. M. BUENO*, J. M. MARTINEZ-DUART

Dpto. Física Aplicada, Facultad de Ciencias, C-XII, Universidad Autónoma de Madrid, Cantoblanco, 28049 Madrid, Spain

MANUEL HERNÁNDEZ-VÉLEZ

Dpto. de Física, I.S.P. "E.J. Varona", C. Libertad, Marianao, C. de la Habana, Cuba

L. VÁZQUEZ

Instituto de Ciencia de Materiales, C.S.I.C., Madrid, Spain

The optical and structural properties of r.f. sputtered CeO₂ thin films deposited on Pyrex substrates have been studied as a function of substrate temperature during deposition. The refractive index, n , extinction coefficient, k , and bandgap of the films were calculated from reflectance, R , and transmittance, T , spectra in the wavelength range 340–900 nm. The refractive index of CeO₂ films at 550 nm comprises values from about 2.25–2.4 depending on the substrate temperature during deposition. The extinction coefficient was negligible for wavelength values higher than 400 nm. The value obtained for the bandgap was 3.1 eV. The X-ray diffraction patterns showed the same (f c c) cubic structure with preferential orientation depending on substrate temperature during deposition. The scanning force microscope measurements showed that the roughness and grain size of the CeO₂ films increase with increasing substrate temperature.

1. Introduction

In recent years, the deposition techniques and physical properties of cerium dioxide (CeO₂) thin films on different substrates have been increasingly investigated due to its applications in optical devices as a high refractive index material in single and multi-layer coatings [1]. On the other hand, CeO₂ is also used in silicon-on-insulator structures (SOI), buffer layers and capacitor devices [2, 3].

Cerium dioxide films show high transmission in the visible and infrared regions, good adhesion and a very sharp optical absorption edge. Singh *et al.* [4] investigated the properties of vacuum-evaporated films containing a Group IV oxide co-evaporated with CeO₂ for microelectronic devices. Other authors [5, 6], have performed investigations on the properties of CeO₂ thin films prepared by ion-assisted deposition techniques.

In the present work, we report optical and structural properties as well as the surface morphology of r.f. sputtered CeO₂ thin films on Pyrex substrates, prepared under various experimental conditions. The refractive index, extinction coefficient and bandgap of the films were calculated from transmittance, T , and reflectance, R , spectra. There exist several methods to extract the optical constants from R – T

measurements [7]. In this work we have used a method recently developed by us [8] whose advantages are described in the next section. X-ray diffraction and scanning force microscope (SFM) measurements were used to determine the structural properties and surface morphology of the films, respectively.

2. Experimental procedure

Cerium dioxide films were deposited on Pyrex substrates by r.f. sputtering (Ion Tech B315 planar magnetron) from a CeO₂ target (CERAC Inc, 99.9% nominal purity, diameter 4.4×10^{-2} m) in a highly pure argon atmosphere. The deposition pressure was 2×10^{-3} torr (1 torr = 133.322 Pa) and the r.f. power 40 W. Before each deposition, the substrates were placed in a pure acetone solution and stirred for 10 min. The samples labelled A, B and C, were deposited at 25, 140 and 250 °C substrate temperatures, respectively.

The spectral transmittance and reflectance were measured using a Hitachi 150–20 spectrophotometer, provided with an integrating sphere, in the wavelength interval 300–900 nm. The R – T method used in this work is based in a technique recently developed [8] which provided a reliable and accurate

* Author to whom all correspondence should be addressed.

representation of the optical constants, because it does not make use of the usual approximations such as homogeneous layers, semi-infinite substrate, normal incidence angle for reflectance measurements, etc. The method is based on the criteria of continuity and smoothness of the optical constants.

Stylus profilimeter measurements (Dektak 3030) were made to obtain the film thickness. The values obtained were 310, 370 and 340 nm for A, B and C, respectively.

The X-ray diffraction patterns were obtained from a Siemens D5000 diffractometer using $\text{CuK}\alpha$ radiation from 24° – 63° .

Roughness measurements were made with a commercial SFM microscope from Digital Instruments (Nanoscope III) operating in the contact mode (force used ~ 10 nNw) and using silicon nitride cantilevers.

3. Results and discussion

3.1. Optical properties

Fig. 1 shows the experimental reflectance, R , and transmittance, T , spectra of CeO_2 thin films on Pyrex substrates. The optical behaviour of the samples is shown in Fig. 2. As can be observed, the refractive index is clearly dependent on the substrate temperature during deposition. The increase of the refractive index is related to a higher density of the film as the deposition temperature increases. Table I gives the refractive index of CeO_2 films at 550 nm as a function of substrate temperature. Other authors observed similar behaviour for CeO_2 thin films deposited by different techniques [1, 5]. However, the values of the refractive index of the films deposited by sputtering are somewhat higher compared with the case of electron-beam evaporation. For instance, Al-Robaee *et al.* [1] obtained values for the refractive index of CeO_2 thin films by electron-beam evaporation from 1.90–2.29 as the substrate temperature increased from ambient to 300°C . The extinction coefficient (Fig. 2) for all substrate temperatures showed the same values in the strong absorption region (360–320 nm). This is in agreement with the behaviour of the optical bandgap

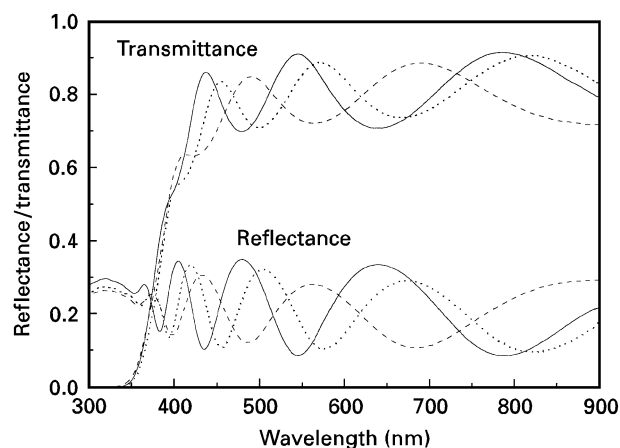


Figure 1 Reflectance and transmittance of CeO_2 thin films deposited on Pyrex substrates at different temperatures. (---) Sample A, $T = 25^\circ\text{C}$; (-.-) sample B, $T = 140^\circ\text{C}$; (—) sample C, $T = 250^\circ\text{C}$.

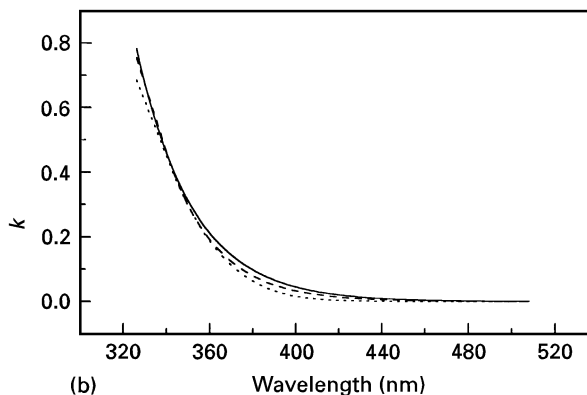
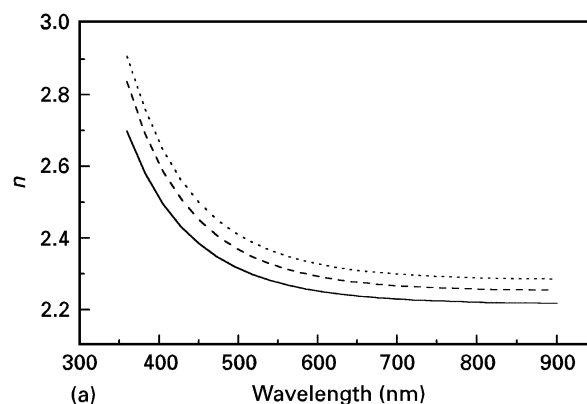


Figure 2 (a) Refractive index, n , and (b) extinction coefficient, k , of CeO_2 thin films as a function of substrate temperature. (—) Sample A, $T = 25^\circ\text{C}$; (-.-) sample B, $T = 140^\circ\text{C}$; (---) sample C, $T = 250^\circ\text{C}$.

TABLE I Refractive index and bandgap of CeO_2 films as a function of substrate temperature

| Sample | Temperature ($^\circ\text{C}$) | Refractive index (at 550 nm) | Bandgap (eV) |
|--------|----------------------------------|------------------------------|--------------|
| A | 25 | 2.276 | 3.14 |
| B | 140 | 2.319 | 3.16 |
| C | 250 | 2.358 | 3.12 |

calculated for these films as can be observed in Table I. These values for the bandgap were obtained from the relation given by Davis and Mott [9] for non-direct transitions

$$\alpha E = A(E - E_{\text{gap}})^2 \quad (1)$$

where α is the absorption coefficient, E the photon energy, E_{gap} the optical bandgap and A is a constant. Representing $(\alpha E)^{1/2}$ as a function of E leads to a linear behaviour and the extrapolation to the values of $(\alpha E)^{1/2} = 0$ gives E_{gap} . However, in the low absorption region (360–400 nm), the extinction coefficient, k , decreases when the films are deposited at higher substrate temperatures. This is probably due to the lower density of the films deposited at room temperature as a consequence of the larger portion of voids incorporated during the deposition process. The presence of these voids can broaden the energy bands leading to an increase of the interband transitions, and consequently to an increase of the extinction coefficient in the low absorption region. For wavelengths above

TABLE II XRD parameters of the samples

| Sample | Temp. (°C) | (<i>hkl</i>) | 2θ (deg) | FMWH | Intensity (Arb. units) |
|--------|------------|----------------|----------|-------|------------------------|
| A | 25 | 111 | 27.84 | 1.11 | 554.3 |
| | | 220 | 46.33 | 1.77 | 486.39 |
| B | 140 | 111 | 27.939 | 2.188 | 69.23 |
| | | 200 | 32.686 | 0.642 | 376.36 |
| | | 220 | 46.375 | 2.158 | 323.88 |
| C | 250 | 111 | 27.991 | 3.149 | 177.8 |
| | | 200 | 32.647 | 1.015 | 93.697 |
| | | 220 | 46.407 | 1.411 | 900.79 |

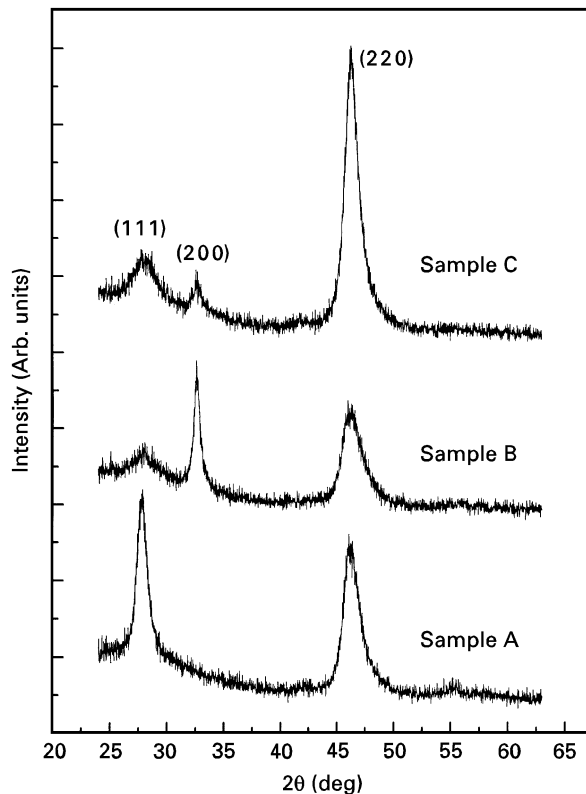


Figure 3 X-ray diffraction patterns of the samples. Sample A, $T = 25^\circ\text{C}$; sample B, $T = 140^\circ\text{C}$; sample C, $T = 250^\circ\text{C}$.

400 nm, the extinction coefficient remains negligible ($< 10^{-3}$) for the different CeO_2 films.

3.2. Structural characterization

All the CeO_2 films investigated in this work show the cubic (fcc) crystalline structure as can be deduced from Fig. 3. These patterns show that the texture of the CeO_2 films changed as the temperature increased from 25°C to 250°C . Table II shows the results obtained from the XRD analysis of the peaks after adjustment to Lorentzian curves. The most important reflection was obtained from the (220) crystallographic planes in sample C which was deposited at the highest substrate temperature. From the figure, it is clear that the texture of the films deposited at room temperature, faced (111) and (220) with approximately the same proportion, evolves to a strongly textured (220) film when the substrate temperature was 250°C . This feature is in accordance with those

TABLE III Lattice constant, calculated from Table II, of CeO_2 films as a function of substrate temperature

| Sample | Temperature (°C) | Lattice constant (nm) |
|--------|------------------|-----------------------|
| A | 25 | 0.554 |
| B | 140 | 0.551 |
| C | 250 | 0.550 |

reported by other authors who have deposited this kind of material by other techniques using higher substrate temperatures and different atmospheres [1, 3]. However, a singular behaviour was found in the main reflections of film B, which could be attributed to a recrystallization process during deposition [1]. The feature observed in sample B for (200) reflection probably indicates that the films can be grown with this preferential orientation in a shorter substrate temperature range between 50 and 250°C . From Table III, it is also noticeable that the lattice constant decreases as the substrate temperature increases. Consistently, for the film deposited at the highest substrate temperature (250°C), we obtained both the highest crystal density and refractive index, as mentioned above. This fact also suggests an increase in the grain size with substrate temperature, which agrees with the results from the SFM micrographs, which are shown below.

3.3. Surface morphology

In order to characterize the surface morphology of CeO_2 films, SFM images were obtained in different regions of the samples and different areas (0.25 , 1 and $4 \mu\text{m}^2$). Fig. 4 corresponds to various typical $1 \mu\text{m}^2$ three-dimensional images of the samples (the z -scale is the same in the three micrographs). All the images show a granular structure with the mean grain size increasing with the deposition temperature. This is confirmed after obtaining the grain-size distribution of the surface by a statistical analysis of the images with the SFM software. Fig. 5 shows the mean and grain-size distribution for the three samples. The average grain size increases from 67.7 nm for sample A to 89.1 nm for sample C. This is in agreement with the XRD measurements that showed the lowest value of the full-width at half-maximum in the [220] orientation for the sample C deposited at the highest substrate temperature.

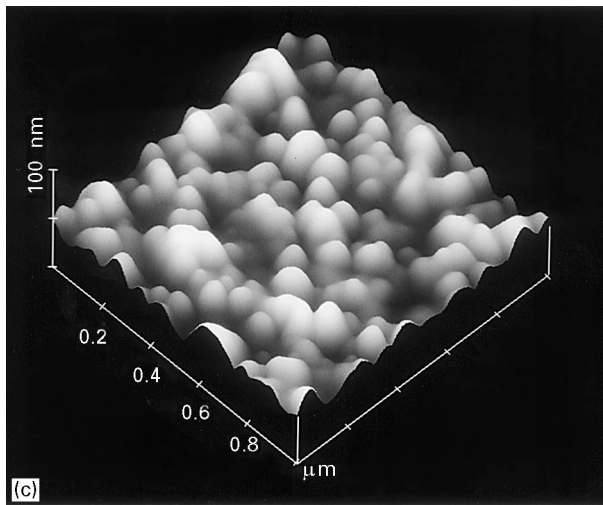
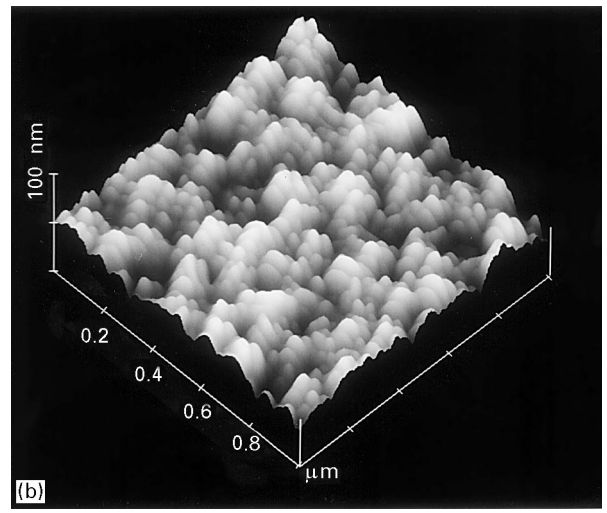
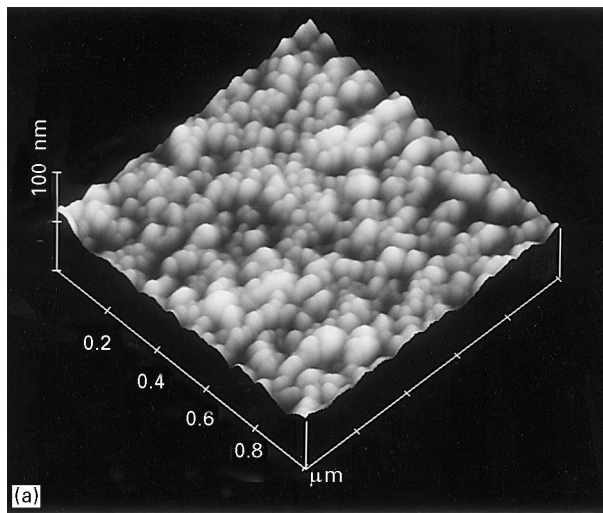


Figure 4 $1 \mu\text{m}^2$ three-dimensional SFM images of samples: (a) A, (b) B and (c) C. Note that the z-scale is the same in all images (50 nm div^{-1}).

TABLE IV Roughness of CeO_2 films as a function of substrate temperature

| Temperature ($^{\circ}\text{C}$) | SFM Average roughness (nm) |
|------------------------------------|----------------------------|
| 25 | 2.9 |
| 140 | 6.5 |
| 250 | 7.5 |

It is observed from Fig. 4 that the film surface roughness increases with the deposition temperature. SFM software also allows the surface roughness to be quantified directly from the SFM images. Thus, by averaging the root mean square (rms) roughness of several $1 \mu\text{m}^2$ images, we obtain the results for the three films reported in Table IV. The surface roughness of the uncoated Pyrex substrate was previously measured and the average value was 0.3 nm. As a result of the SFM observations, the increase of rms surface roughness can be related to a larger grain which results when the substrate temperature increases.

4. Conclusion

Cerium dioxide CeO_2 thin films deposited by r.f. sputtering on Pyrex substrates have been characterized as

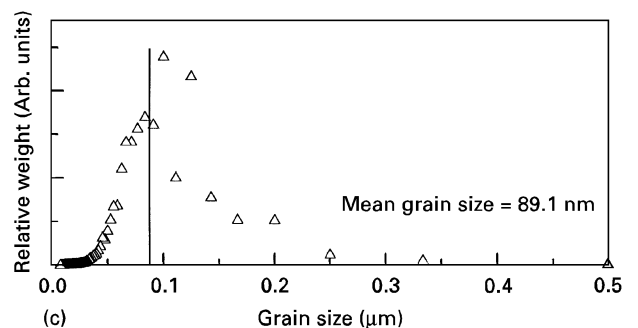
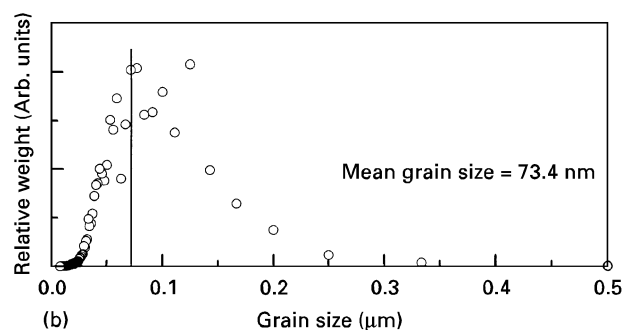
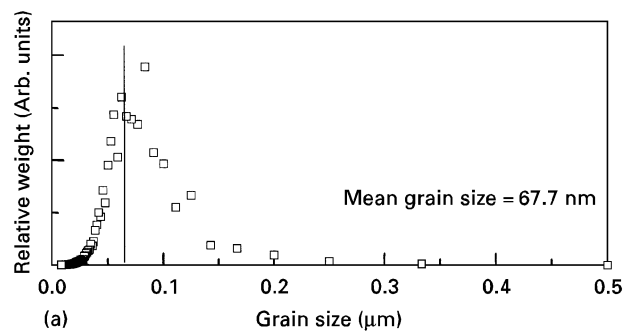


Figure 5 Grain-size distribution for samples (a) A, (b) B and (c) C. The mean grain size is marked by a vertical line. Sample A, $T = 25^{\circ}\text{C}$; sample B, $T = 140^{\circ}\text{C}$; sample C, $T = 250^{\circ}\text{C}$.

a function of substrate temperature. The refractive index, n , has been observed to be strongly dependent on substrate temperature, whereas similar values of the extinction coefficient, k , and bandgap were obtained for all the films. The obtained thin films showed high n values along with very low k values.

From the XRD analysis, the main observed effect is the increase in the (220) reflections for the highest substrate deposition temperature, suggesting an increase of the texture of the films in that direction by the temperature effect. On the other hand, SFM measurements indicated the increment of surface roughness and grain size with substrate temperature increase.

Acknowledgements

We thank IBERDROLA and the Brite Euram Program (Project 5528-92) of the European Community for financial support. One of the authors (MHV) thanks the Education and Science Ministry of Spain for a grant supported by the programme "Estancias Temporales de Científicos y Tecnólogos Extranjeros en España".

References

1. M. S. AL-ROBAEE, K. NARASIMHA RAO and S. MOHAN, *J. Appl. Phys.* **71** (1992) 2380.
2. T. INOUE, M. OSONOE, H. TOHDA and M. HIRAMATSU, *ibid.* **69** (1991), 8313.
3. T. INOUE, T. OHSUNA, L. LUO, X. D. WU, C. J. MAGGIONE, Y. YAMAMOTO, Y. SAKURAI and J. H. CHANG, *Appl. Phys. Lett.* **59** (1991) 3604.
4. A. SINGH, E. A. DAVIS, S. J. GURMAN and C. A. HOGARTH, *J. Mater. Sci.* **24** (1989) 2623.
5. R. P. NETTERFIELD, W. G. SAINTY, P. J. MARTIN and S. H. SIE, *Appl. Opt.* **24** (1985) 2267.
6. M. S. AL-ROBAEE, M. G. KRISHNA, K. N. RAO and S. MOHAN, *J. Vac. Sci. Technol. A* **9** (1991), 3048.
7. D. P. ARNDT, R. M. A. AZZAM, J. M. BENNETT, J. P. BORGOGNO, C. K. CARNIGLIA, W. E. CASE, J. A. DOBROWOLSKI, U. J. GIBSON, T. TUTTLE HART, F. C. HO, V. A. HODGKIN, W. P. KLAPP, H. A. MACLEOD, E. PELLETIER, M. K. PURVIS, D. M. QUINN, D. H. STROME, R. SWENSON, P. A. TEMPLE and T. F. THONN, *Appl. Opt.* **23** (1984), 3571.
8. R. M. BUENO, J. F. TRIGO, J. M. MARTINEZ-DUART, E. ELIZALDE and J. M. SANZ, *J. Vac. Sci. Technol. A* **13** (1995) 1.
9. E. A. DAVIS and N. F. MOTT, *Philos. Mag.* **22** (1970) 903.

*Received 22 September 1995
and accepted 18 March 1996*